Received: 8 March 2022 | Revised: 16 September 2022 | Accepted: 21 September 2022

DOI: 10.1111/cas.15627

Cancer Science WILEY

ORIGINAL ARTICLE

Diallyl trisulfide alleviates chemotherapy sensitivity of ovarian cancer via the AMPK/SIRT1/PGC1α pathway

Zhaojun Wang[1] | Yi Yan[1] | Yijie Lou[1,2] | Xiaoyan Huang[3] | Lijian Liu[3] | Zhuofan Weng[1] | Yusheng Cui[1] | Xinyue Wu[1] | Huijun Cai[1] | Xiaohui Chen[1] | Yunxi Ji[4]

[1]The First School of Clinical Medicine, Zhejiang Chinese Medical University, Hangzhou, China

[2]Key Laboratory of Digestive Pathophysiology of Zhejiang Province, Hangzhou, China

[3]Department of Spleen and Gastric Diseases, The First Affiliated Hospital of Guangxi University of Chinese Medicine, Guangxi, China

[4]Department of General Practice, The First Affiliated Hospital of Zhejiang Chinese Medical University, Hangzhou, China

Correspondence
Yunxi Ji, Department of General Practice, The First Affiliated Hospital of Zhejiang Chinese Medical University, No. 54, Youdian Road, Shangcheng District, Hangzhou 310006, Zhejiang, China.
Email: jyx1832@126.com

Funding information
National Natural Science Foundation of China, Grant/Award Number: 81260531 and 81873268

Abstract

Platinum-based chemotherapy promotes drug resistance in ovarian cancer. We investigated the antichemoresistance characteristics of diallyl trisulfide (DATS) in cisplatin-resistant ovarian cancer cells, in vitro and in vivo. Previous preclinical studies have revealed that DATS regulates distinct hallmark cancer-signaling pathways. The cell cycle pathway is the most investigated signaling pathway in DATS. Additionally, post-DATS treatment has been found to promote proapoptotic capacity through the regulation of intrinsic and extrinsic apoptotic pathway components. In the present study, we found that treating cisplatin-sensitive and cisplatin-resistant ovarian cell lines with DATS inhibited their proliferation and reduced their $IC_{50.}$ It induced cell apoptosis and promoted oxidative phosphorylation through the regulation of the AMPK/SIRT1/PGC1α pathway, OXPHOS, and enhanced chemotherapy sensitivity. DATS treatment alleviated glutamine consumption in cisplatin-resistant cells. Our findings highlight the role of DATS in overcoming drug resistance in ovarian cancer in vitro and in vivo. In addition, we elucidated the role of the AMPK/SIRT1/PGC1α signaling pathway as a potential target for the treatment of drug-resistant ovarian cancer.

KEYWORDS
AMPK/SIRT1/PGC1α pathway, cisplatin, drug resistance, ovarian cancer, ROS

1 | INTRODUCTION

Ovarian cancer is one of the most aggressive cancers of the female reproductive system.[1] Globally, more than 200,000 newly diagnosed cases of ovarian cancer are reported each year; the 5-year survival rate is lower than 45%, with 15,000 death cases annually, making ovarian cancer the 8th most common cause of cancer-associated death in women.[2,3] The major contributing factors to this high mortality rate include asymptomatic progression and late diagnosis at an advanced stage in more than 70% of patients.[4] Ovarian cancer treatments

Abbreviations: CCK-8, cell-counting kit-8; DATS, diallyl trisulfide; HCl, hydrochloric acid; HE, hematoxylin and eosin; IP, immunoprecipitation; OD, optical density; OXPHOS, oxidative phosphorylation; PBS, phosphate-buffered saline; PUMA, p53 upregulated modulator of apoptosis; ROS, reactive oxygen species; SKOV-3/DDP, cisplatin-resistant ovarian cancer cells; WB, Western blotting.

Zhaojun Wang, Yi Yan and Yijie Lou contributed equally to this study.

include surgery and subsequent chemotherapy; however, their efficiency is limited.[1] The sensitivity to platinum-based chemotherapy in patients with ovarian cancer is >70%. Half of these patients experience recurrence and peritoneal metastases, leading to low overall survival rates.[5] Consequently, therapeutic resistance in these patients will develop sooner or later toward single or combination chemotherapies.[6] Distinct molecular mechanisms have been suggested to be involved in ovarian cancer chemoresistance, including increased anti-apoptotic activity and altered drug inactivation.[7] However, the exact mechanisms by which ovarian cancer develops cisplatin resistance have yet to be explored. Thus, it is crucial to find anti–drug-resistant, nontoxic, and effective drugs to treat ovarian cancer.

Bioactive dietary agents regulate various cancer-signaling pathways. The consumption of allium vegetables such as garlic and onions decrease cancer incidence. Diallyl trisulfide (DATS), a bioactive compound derived from allium vegetables, is known as an anticancer and chemoresistant agent.[8] Different studies have revealed that DATS can induce cell apoptosis in various cancers, such as colon, lung, skin, and breast cancers.[9–13] DATS has also been reported to regulate p53 upregulated modulator of apoptosis (PUMA) expression and promote apoptosis in cisplatin-resistant ovarian cancer cells (SKOV-3/DDP).[14]

The PGC-1α-AMPK-SIRT1 pathway is involved in the regulation of energy metabolism and mitochondrial biogenesis. Reactive oxygen species (ROS) production can positively induce many transcription coactivators and factors, but its coordinated mechanism is not well studied. Among these transcription factors, PGC-1 α plays a central role in mitochondrial biogenesis and antioxidant boosting via several signaling kinases, including AMPK.[15,16]

Reactive oxygen species are involved in glycolysis dys/regulation and vice versa in cancer and other diseases linked to mitochondrial dysfunction. Exceeded and counterbalanced glucose uptake occurs after glucose-stimulated ROS production triggers a toxic cycle and ultimately leads to cell death.[17] Also, ROS production depends on the used oxidative phosphorylation (OXPHOS) substrates and inhibitors, respectively.[18,19] On the other hand, OXPHOS proteins are regulated by ROS.[20] Generally, if ROS levels exceed a specific limit, they will impair OXPHOS complexes and further stimulate ROS production.[21]

In the present study, the effectiveness of DATS against chemoresistance characteristics was analyzed in cisplatin-resistant and cisplatin-sensitive cell lines in vitro and in vivo. We hypothesize that DATS can overcome cisplatin resistance in ovarian cancer cell lines and animal models by modulating the AMPK/SIRT1/PGC1α signaling pathway, which can promote cell apoptosis and ROS production.

2 | MATERIALS AND METHODS

2.1 | Reagents

Ovarian cancer cell lines (A2780, A2780/DDP, COC1, COC1/DDP) were purchased from Zhejiang Chinese Medical University. The following reagents were used: phosphatase inhibitors (Biyuntian, S1873); CCK8 detection kit (Beyotime, C0037); DATS and cisplatin (Source leaf, B25320, and B24462); annexin VFITC kit (Nanjing KGI Bio, KGA108); glucose test kit (Nanjing built, F006–11); ROS activity detection kit (Nanjing built, E004–11); glutamine and glutamate determination kit (Sigma Aldrich, GLN1); and NAC, OM, AMPK inhibitor compound C, and AMPK activator AICAR (MCE, HYB0215, HYN6782, HY13418, and HY-13417). The following antibodies were used: pAMPK (Bioss, bs4002R); AMPK, SIRT1, and PGC1α (Affinity, DF2656, DF6033, and AF5395); acetylated-lysine (Cell Signaling Technology, 9441); and OXPHOS (Abcam, ab110411). All other reagents were purchased from Sigma Aldrich.

2.2 | Cell-counting kit-8 (CCK-8) assay

Each designated cell line was digested in 0.25% trypsin solution at room temperature for 2 minutes and counted to prepare a cell suspension. The cells were then seeded in a 96-well plate (1000 cells/well), and the cells were treated following each experimental design. The cells were incubated at 37°C, followed by adding the CCK-8 assay (Beijing Solarbio Science & Technology, Co., Ltd.) to determine the cell viability. Each well containing 10 μl CCK-8 reagent was then incubated at 37°C for 1.5 hours. The optical density (OD) values were determined using a microplate reader at 450 nm. Each assay was performed in triplicate.

2.3 | Hematoxylin and eosin (HE) staining

Each tumor specimen was stored in paraffin wax for further analysis. Before HE staining, the specimen was dewaxed in xylene I (10 minutes) and xylene II (5 minutes) and then dehydrated in 100% alcohol I (5 minutes), 100% alcohol II (5 minutes), 95% alcohol I (5 minutes), 95% alcohol II (5 minutes), 85% alcohol (3 minutes), and 75% alcohol (2 minutes), followed by rinsing with distilled water (1 minutes). Further, the specimens were immersed in hematoxylin dye solution for 5-20 minutes, rinsed with tap water for 3-5 minutes, followed by 1% hydrochloric acid (HCl)-alcoholic differentiation for 1-5 seconds. The specimens were then rinsed with tap water for 1-3 minutes, stained with 1% eosin alcohol for 1 minutes, and washed with distilled water for 2 minutes. Further, the specimens were dehydrated with 75% alcohol (2 minutes), 85% alcohol (2 minutes), 95% alcohol I (5 minutes), 95% alcohol II (5 minutes), 100% alcohol I (5 minutes), and 100% alcohol II (5 minutes). Following dehydration, the specimens were submerged in xylene I and xylene II for 5 minutes each and mounted on microscope slides for imaging.

2.4 | TUNEL assay and Ki67 staining assay

The specimens were deparaffinized, soaked in xylene for 5 minutes, and sequentially immersed in 100%, 95%, 90%, 80%, and 70% ethanol for 3 minutes. Further, the specimens were soaked

in 3% hydrogen peroxide in methanol for 10-15 minutes to inhibit endogenous catalase and incubated with proteinase K (20 μg/mL dissolved in Tris/HCl, pH 7.48.0) for 15-30 minutes at room temperature. The specimens were washed twice with phosphate-buffered saline (PBS) for 5 minutes each time and dried. The TUNEL reaction mixture was prepared with 100 μl of labeling solution according to the manufacturer's protocol. A total of 50 μl TUNEL reaction mixture was added dropwise and incubated at 37°C in a wet box for 60 minutes. After washing the specimens with PBS three times for 5 minutes each, the samples were analyzed under a fluorescence microscope (green fluorescent protein). Afterward, the samples were dried, and 50 μl transformant-POD was added to each specimen and incubated in a humid box at 37 °C for 20-30 minutes, followed by washing with PBS for 5 minutes, 3-5 times. Further, 50-100 μl DAB substrate solution was added, incubated at room temperature for 5-10 minutes, and washed three times with PBS for 5 minutes each. The samples were then analyzed under a microscope (Upright Optical Microscope, Nikon). Images were analyzed using a chemiluminescence imaging system (Shanghai Ouxiang Scientific Instrument Co., Ltd.).

2.5 | Immunoprecipitation (IP) and gene knockdown

The IP assay has been performed as previously described.[22] For gene knockdown, the corresponding sequence of PGC1α has been synthesized by Zhejiang Chinese Medical University. Briefly, the cells were transfected with si-PGC1α using Lipofectamine 3000 (Invitrogen) following the manufacturer protocol. The cells were treated accordingly for 48 hours post transfection, and then the cell viability and protein expression were detected.

2.6 | Flow cytometry

The annexin V-FITC and PI double-staining has been used to detect the apoptosis rate in control and post-treated cells. The cells were digested using trypsin without EDTA, washed by PBS twice, and centrifuged at 2000 rpm for 5 minutes. Then, the cells were collected into the flow cytometer tubes for further analysis.

2.7 | Western blotting (WB)

The protein expressions of OXPHOS, SIRT1, PGC1α, p-AMPK, and AMPK in the cell lines and tumor tissue samples were detected by WB. The cells were collected, and total protein was extracted and quantified using the Bradford method. The lysates (30 μg of protein for each well) were electrophoresed on an SDS-PAGE gel for 4 hours before blotting onto PVDF membranes. These blots were then incubated with primary antibodies overnight at 4°C. The next day, the membranes were washed and incubated for 1.5 hours with a horseradish peroxidase–conjugated secondary antibody. After incubation with the secondary antibodies, the membranes were washed and developed using an ECL system. Protein expression levels were determined by analyzing the signals captured on the membranes using Image-Pro Plus 6.0 analysis software (Media Cybernetics, Inc.). B-actin was used as an internal control. Further, PGC1α was extracted using IP assay and incubated with an acetylated lysine antibody. Acetylation of PGC1α was detected by WB.

2.8 | Determination of glutamine level, glucose level, and ROS level

Glutamine level was detected using the glutamine and glutamate determination kit according to the manufacturer's protocol. OD value was measured at 339 nm wavelength.

Glucose level was detected using the glucose test kit according to the manufacturer's protocol.

ROS level was measured using the ROS activity detection kit according to the manufacturer's protocol. The results were quantified using the fluorescence intensity.

2.9 | In vivo analysis

Nude mice were injected with A2780/DDP cells (2×10^6, 0.2 ml PBS) subcutaneously into the armpit of the right forelimb to construct a transplanted tumor model. When the tumor grew to a size of $100\times150\,mm^3$, the mice were randomly divided into four groups; each group was administered one of the following antitumor agents: cisplatin (3 mg/kg, ip), once every 5 days, a total of three times; DATS (20 mg/kg, ip), once a day; corresponding PBS volume in the control group; and sulfur suspension (200 mg/kg, 1050 mg), intragastrically, once a day. Additionally, the length and width of the tumors and the tumor volume was calculated weekly. Further, the weight of the animals was measured, and a weight growth curve was drawn weekly. After the mice were sacrificed, part of the tumor tissue was stored at −80°C for WB detection, and part was used for HE staining, TUNEL staining, and ki67 staining assay. Furthermore, the tumors were stripped, photographed, and weighed, and the tumor inhibition rate was calculated. Tumor inhibition rate: IR (%) = $(W_X\times W_{Control})/W_{Control}\times100\%$; W_X is the tumor weight in the same cell line administration group.

2.10 | Combination index (CI) calculation

The CI was calculated using the formula: (Am)50/(As)50 + (Bm)50/(Bs)50. Among them, (Am)50 and (Bm)50 were the IC50 concentrations of cisplatin and DATS in combination. (As)50 and (Bs)50 were the IC50 concentration of cisplatin and DATS alone. CI > 1 indicates antagonism; CI < 1 indicates synergy; and CI = 1 indicates an additive effect.

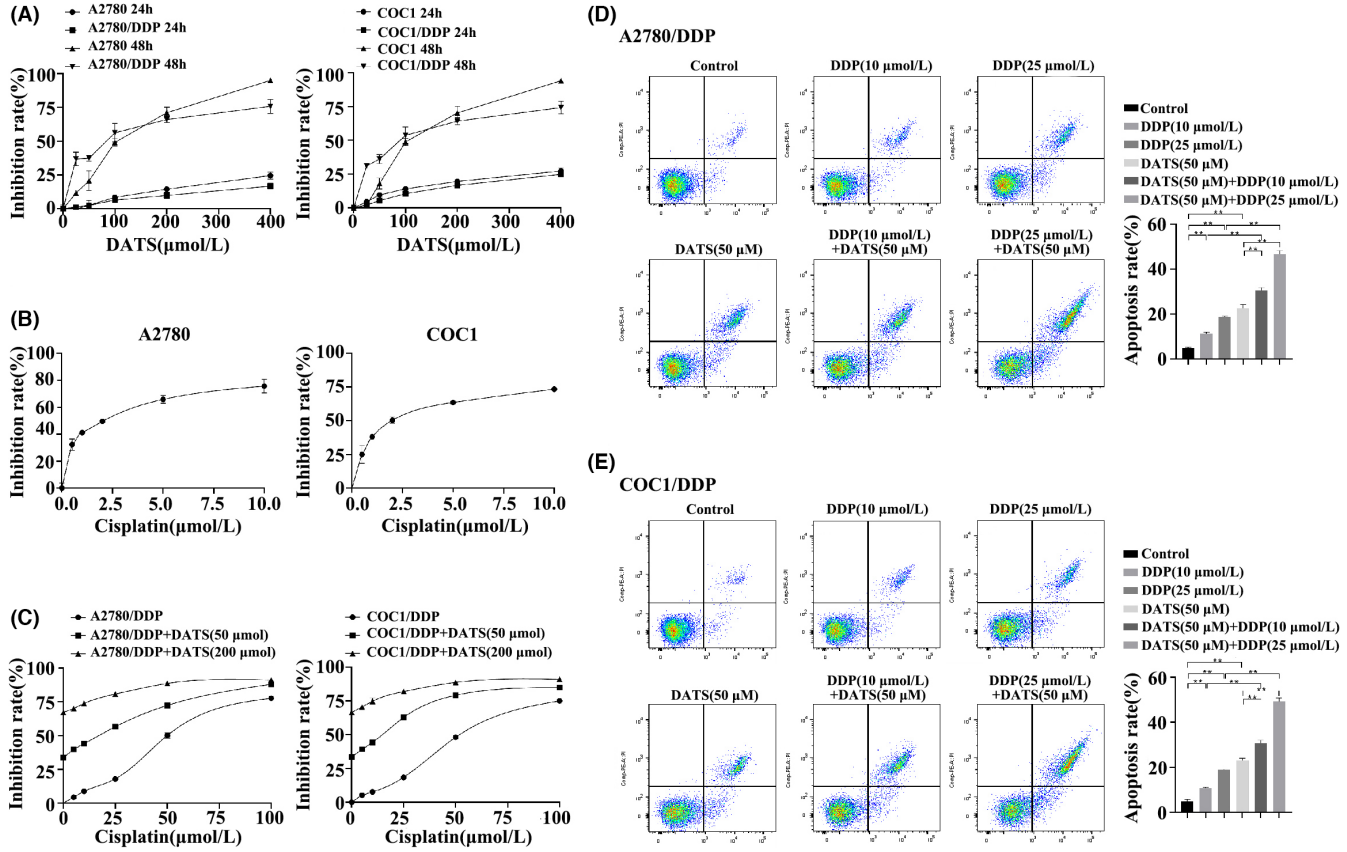

FIGURE 1 Role of diallyl trisulfide (DATS) in inhibiting cisplatin-resistant ovarian cancer cell growth and promoting cell apoptosis. A, The inhibition rates of cisplatin-resistant ovarian cancer cells after treatment with DATS were detected by CCK-8. B, The inhibition rates of ovarian cancer cells after treatment with cisplatin were detected by CCK-8. C, The inhibition rates of cisplatin-resistant ovarian cancer cells after treatment with DATS and cisplatin were detected by CCK-8. D, The apoptosis rates of A2780/DDP cells were detected using flow cytometry. E, The apoptosis rates of COC1/DDP cells were detected using flow cytometry. $^{**}p < 0.01$.

2.11 | Statistical analysis

All results were presented as mean ± SD. Statistical analyses were performed using the GraphPad Prism software (GraphPad Software Inc.). One-way analysis of variance was used for comparisons between different groups. Differences were considered statistically significant at $p < 0.05$.

TABLE 1 The combination index (CI) value of DDP with DATS (48 h)

Cell line	CI value
A2780	0.86
COC1	0.84
A2780/DDP	0.75
COC1/DDP	0.71

3 | RESULTS

3.1 | Role of DATS in inhibiting cisplatin-resistant ovarian cell growth and promoting cell apoptosis

We tested the chemotherapy-resistant effect of DATS on cisplatin-resistant and cisplatin-sensitive ovarian cancer cells. DATS inhibited the growth of the A2780, A2780/DDP, COC1, and COC1/DDP cell lines in a dose- and time-dependent manner (Figure 1A). Treatment of A2780/DDP and COC1/DDP cells with DATS increased their sensitivity to cisplatin and reduced their IC_{50} value (Figure 1B,C). It also induced apoptosis in A2780, A2780/DDP, COC1, and COC1/DDP cells in a dose- and time-dependent manner (Figure 1D,E). The CI value of DATS and DDP were all less than 1, suggesting a synergistic effect between these two drugs in A2780, A2780/DDP, COC1, and COC1/DDP cells (Table 1).

3.2 | Effect of DATS treatment on OXPHOS, ROS expression, and consumption of glucose and glutamine

Considering the vital role of ROS in apoptosis induction, we examined the effect of DATS on ROS and its regulated OXPHOS during glucose uptake. DATS can increase OXPHOS levels in cisplatin-sensitive

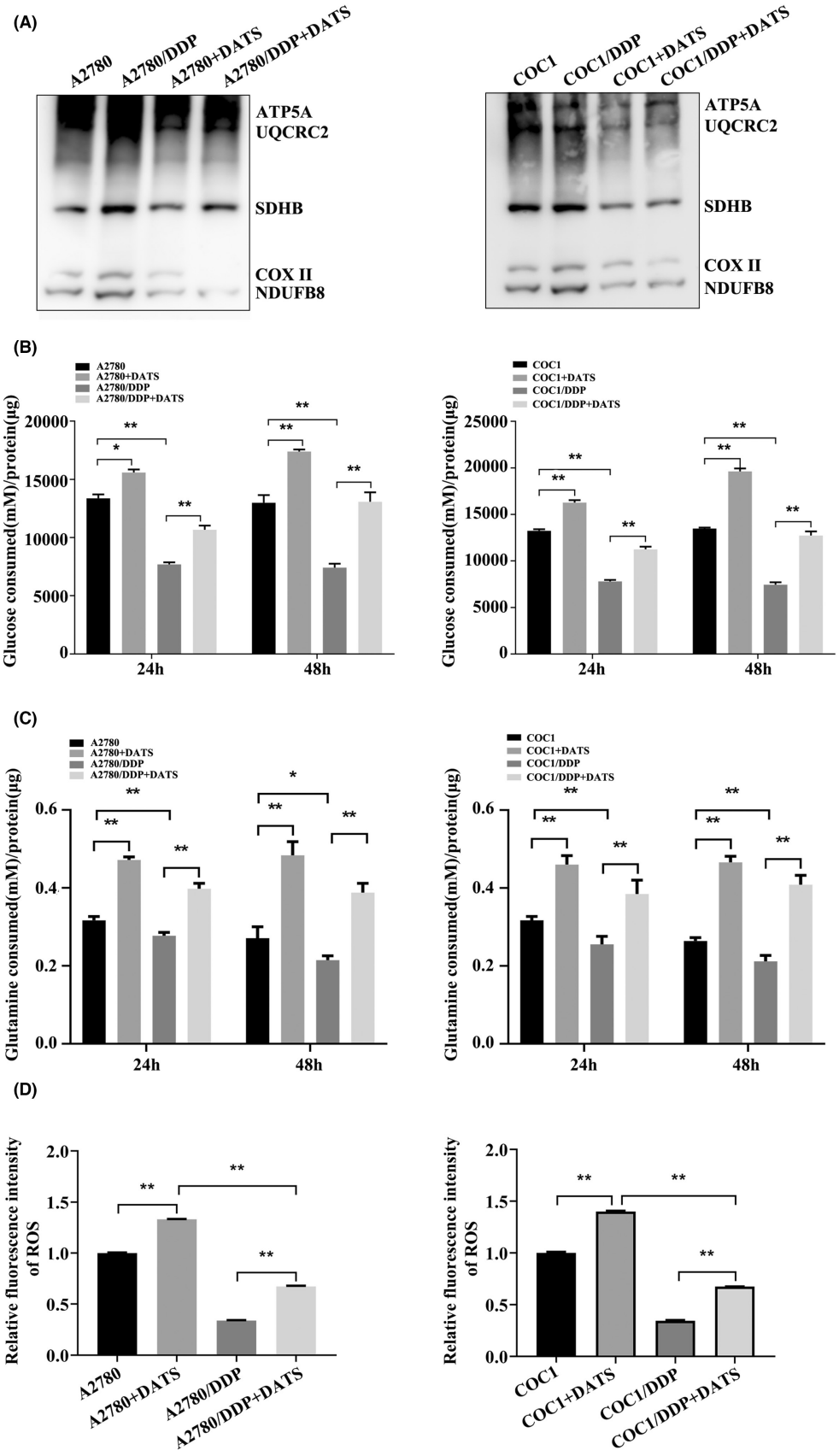

FIGURE 2 Effect of diallyl trisulfide (DATS) treatment on oxidative phosphorylation (OXPHOS), reactive oxygen species (ROS) expression, and glucose and glutamine consumption. A, The protein expression of total OXPHOS in DATS-treated A2780, A2780/DDP, COC1, and COC1/DDP cells. B, The glucose consumption of cisplatin-sensitive or cisplatin-resistant ovarian cancer cells treated with DATS. C, The glutamine consumption of cisplatin-sensitive or cisplatin-resistant ovarian cancer cells treated with DATS. D, The release of ROS in cisplatin-sensitive or cisplatin-resistant ovarian cancer cells treated with DATS. $^{**}p < 0.01$.

and cisplatin-resistant cells compared with those in untreated cells (Figure 2A). DATS treatment also promoted glucose and glutamine consumption in both cisplatin-sensitive and cisplatin-resistant cells (Figure 2B,C). Additionally, DATS elevated ROS levels in cisplatin-sensitive and cisplatin-resistant cells compared with those in untreated cells (Figure 2D).

3.3 | Obstruction of the effects of DATS on cisplatin-sensitive and cisplatin-resistant ovarian cancer cells by OXPHOS inhibitors

DATS can increase the ROS levels; we used the oxidation inhibitors oligomycin (OM) and N-acetyl-L-cysteine (NAC) to determine whether DATS can regulate cell viability and apoptosis by mediating OXPHOS in cisplatin-sensitive or cisplatin-resistant ovarian cancer cells. As shown in Figure 3A,D, cotreatment with DATS and OM or NAC reversed the inhibitory effect of DATS on the viability of cisplatin-sensitive or cisplatin-resistant ovarian cancer cells. In addition, DATS promoted apoptosis and ROS levels, whereas OM or NAC reversed the apoptotic induction rate and ROS production levels in cisplatin-sensitive and cisplatin-resistant ovarian cancer cells (Figure 3B,C,E, and F).

3.4 | Upregulation of the AMPK/SIRT1/PGC1α signaling pathway and inhibition of PGC1α acetylation by DATS

The AMPK/SIRT1/PGC1α signaling pathway is closely associated with ROS level regulation,[15] and acetylation of the PGC1α protein regulates its activity.[23] We examined the effect of DATS on the AMPK/SIRT1/PGC1α signaling pathway and the acetylation of PGC1α protein. DATS increased the protein expression

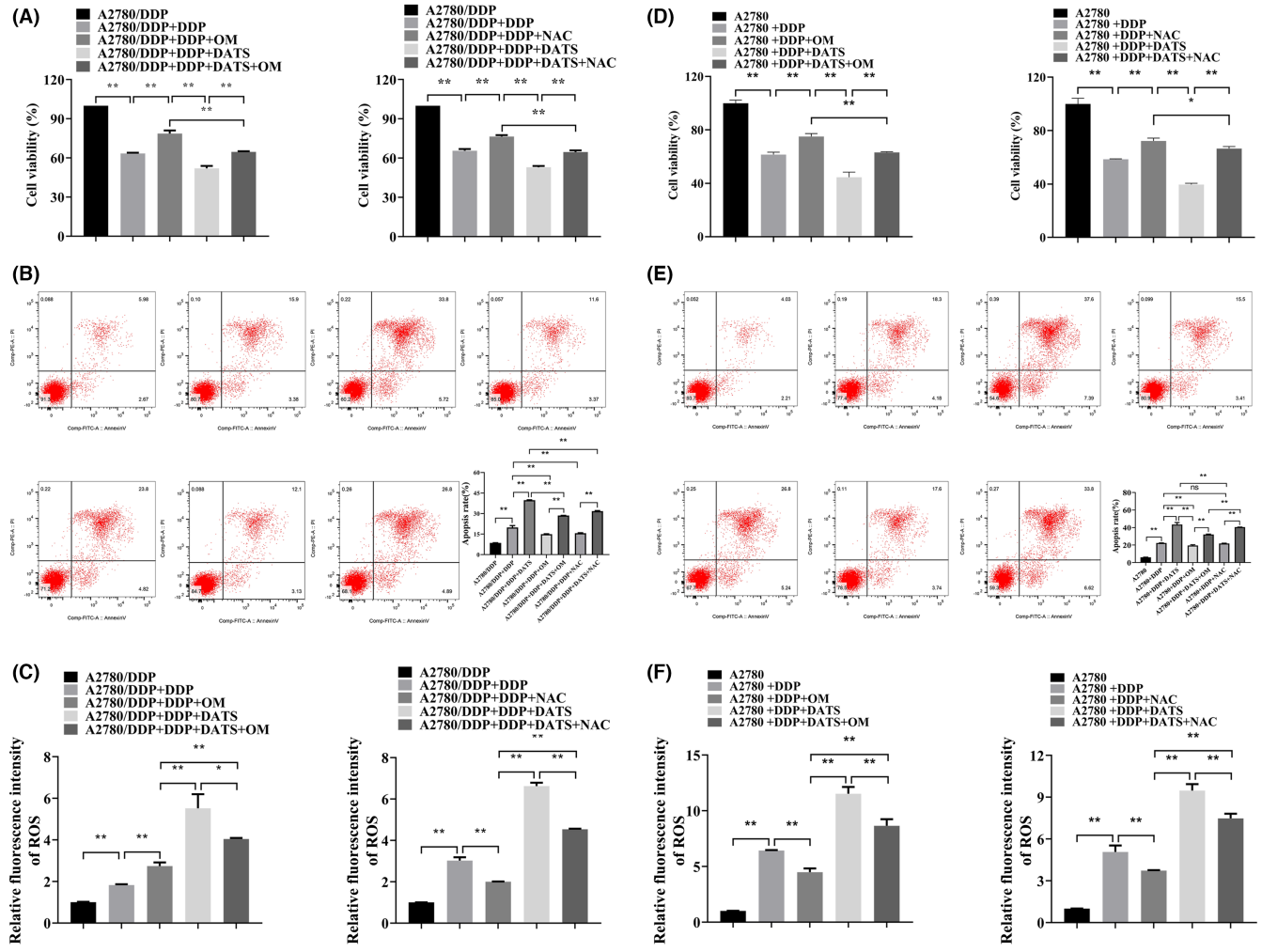

FIGURE 3 Obstruction of the effects of diallyl trisulfide (DATS) in cisplatin-sensitive or cisplatin-resistant ovarian cancer cells by oxidative phosphorylation (OXPHOS) inhibitors. A, The cell viability of A2780/DDP and A2780 cells treated with DATS and oligomycin (OM) or N-acetyl-L-cysteine (NAC) was detected using CCK-8 assay. B, The apoptosis rates of A2780/DDP and A2780 cells were detected using flow cytometry. C, The release of reactive oxygen species (ROS) in A2780/DDP and A2780 cells. D, The cell viability of A2780 cells treated with DATS and NAC or OM were assessed using CCK-8 assay. E, Flow cytometry was used to detect apoptosis rates of A2780 cells. F, The release of ROS in A2780 cells. *$p < 0.05$. **$p < 0.01$.

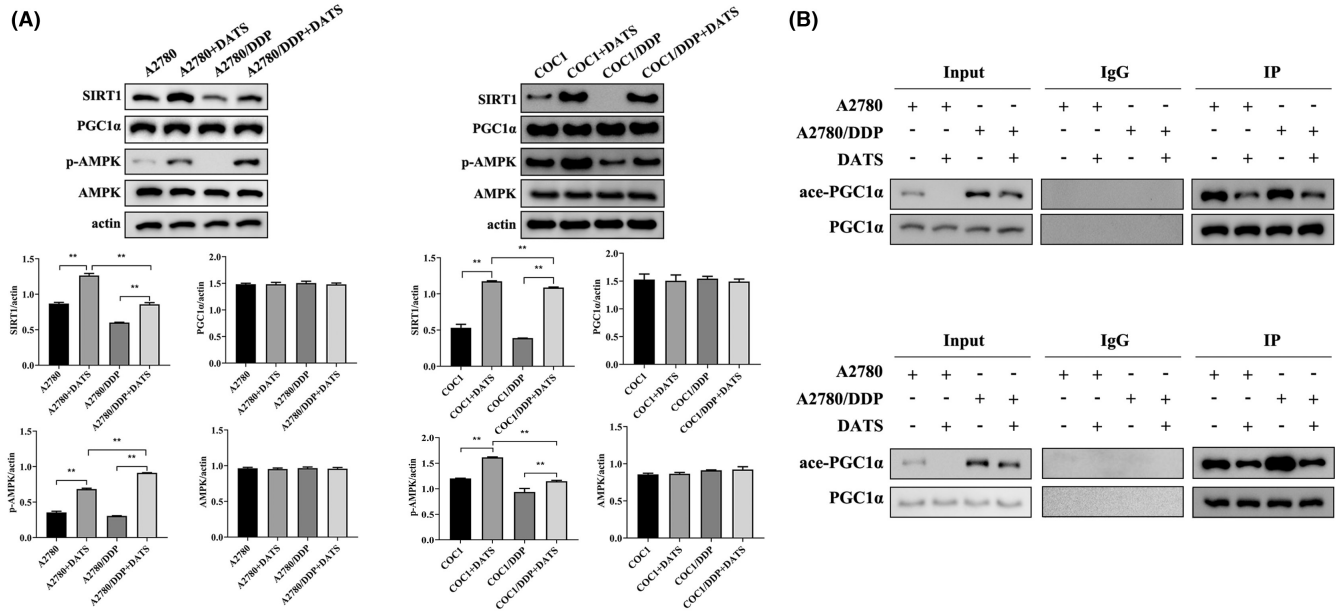

FIGURE 4 Upregulation of the AMPK/SIRT1/PGC1α signaling pathway and inhibition of PGC1α acetylation by diallyl trisulfide (DATS). A, The protein expression of SIRT1, PGC1α, and AMPK in A2780, A2780/DDP, COC1, and COC1/DDP cells was detected using Western blot. B, PGC1α acetylation in A2780, A2780/DDP, COC1, and COC1/DDP cells was detected using Western blot followed by immunoprecipitation (IP) assay. $^{*}p<0.05$, $^{**}p<0.01$, $^{***}p<0.001$.

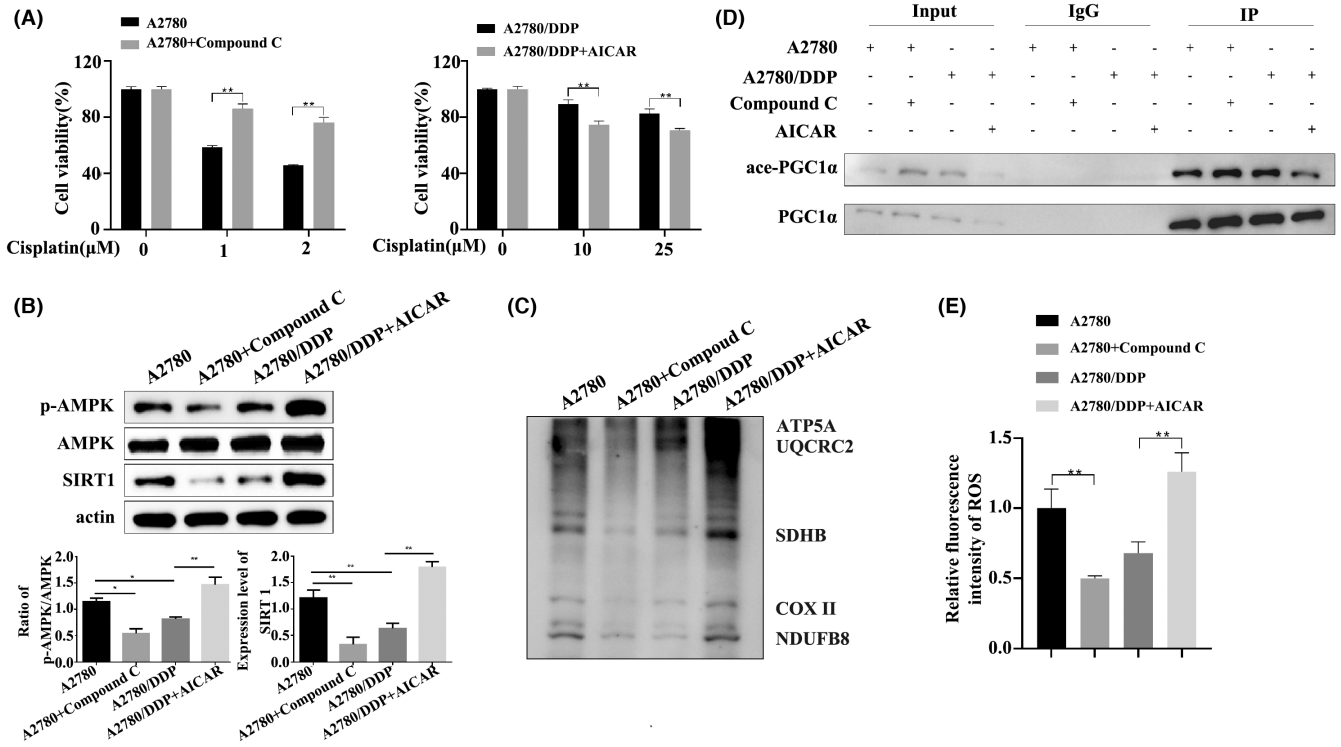

FIGURE 5 Association of AMPK and PGC1α with the regulation of reactive oxygen species (ROS) production and ovarian cancer cell cisplatin sensitivity. A, The cell viability of A2780 and A2780/DDP cells was detected using CCK-8. B, The protein expression of p-AMPK, AMPK, and SIRT1 in A2780 and A2780/DDP cells was detected using Western blot. C, The protein expression of total oxidative phosphorylation (OXPHOS) was detected by Western blot. D, PGC1α acetylation in A2780 and A2780/DDP cells was detected using Western blot followed by immunoprecipitation (IP) assay. E, The release of ROS in ovarian cancer cells. $^{*}p<0.05$; $^{**}p<0.01$.

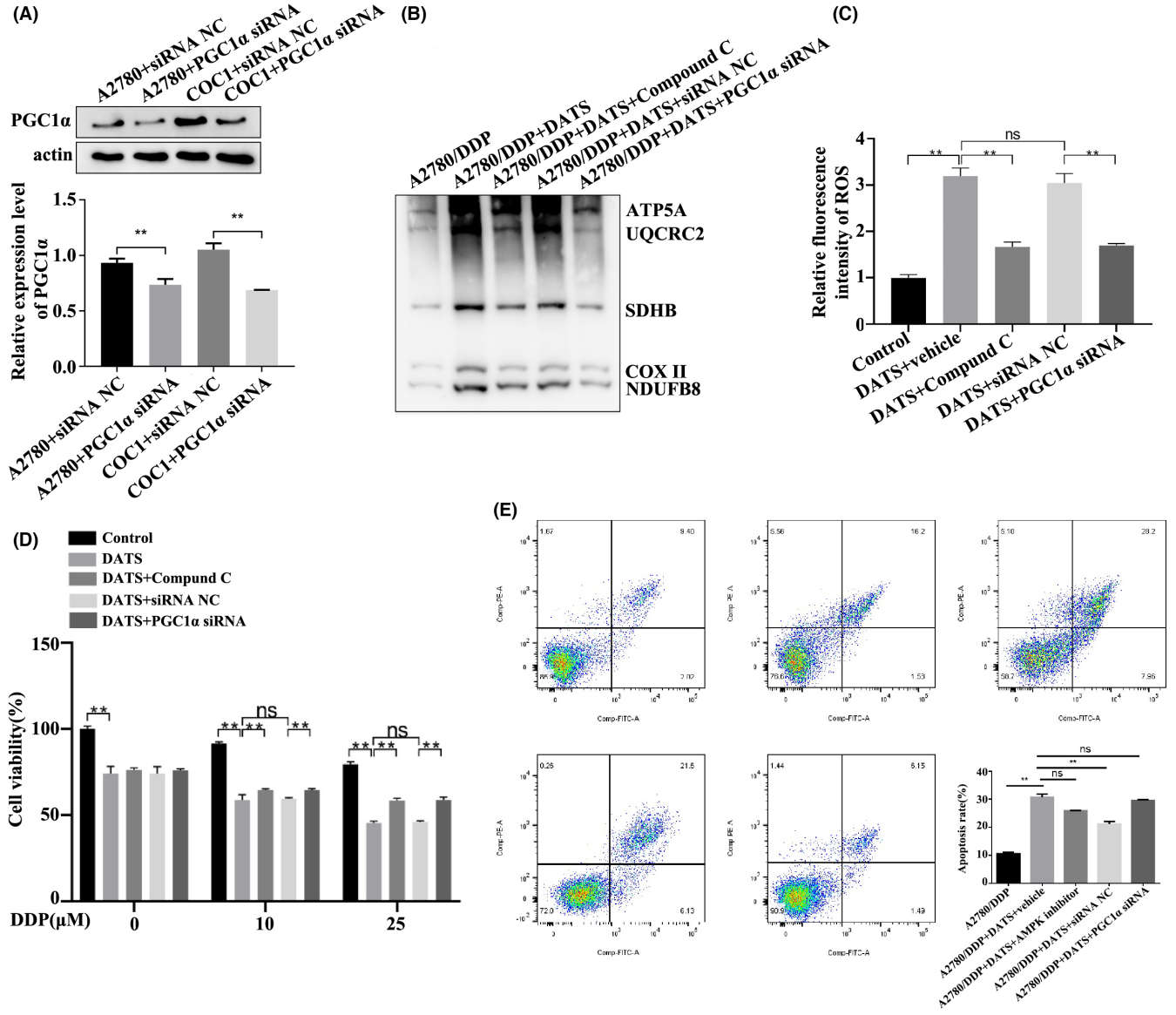

FIGURE 6 Requirement of the AMPK/PGC1α axis for diallyl trisulfide (DATS) activity in cisplatin-resistant ovarian cancer cells. A, The transfection efficiency of PGC1α siRNA was performed using Western blot. B, The protein expression of total oxidative phosphorylation (OXPHOS) was detected by Western blot. C, The release of reactive oxygen species (ROS) in ovarian cancer cells. D, Cell viability following DATS treatment and PGC1α knockdown was detected using CCK-8. E, The apoptosis following DATS treatment and PGC1α knockdown was determined by flow cytometry. $^{**}p < 0.01$. ns: no significant difference.

levels of p-AMPK, AMPK, SIRT1, and PGC1α in cisplatin-sensitive and cisplatin-resistant cells compared with those in untreated cells (Figure 4A). In addition, DATS inhibited PGC1α acetylation (Figure 4B).

3.5 | Association of AMPK and PGC1α with the regulation of ROS production and cisplatin sensitivity in ovarian cancer cells

PGC1α is regulated by AMPK, and AMPK-mediated mitochondrial activation requires PGC1α activity.[24] Thus, we examined the relationship between the activation and inhibition of AMPK protein on ovarian cancer cell sensitivity toward cisplatin treatment. As seen in Figure 5A, the inhibition of AMPK protein decreased the cells' sensitivity toward cisplatin treatment, while the activation of the AMPK protein enhanced their sensitivity. Moreover, the activation of the AMPK/SIRT1/PGC1α signaling pathway was increased by activating the AMPK protein, whereas p-AMPK and SIRT1 levels were decreased by inhibiting this pathway (Figure 5B). Total OXPHOS was increased when AMPK was activated in cisplatin-resistant cells, and inhibition of AMPK reduced OXPHOS (Figure 5C). In addition, PGC1α acetylation decreased when AMPK was activated but increased when AMPK was inhibited (Figure 5D). In contrast, ROS levels increased in cisplatin-resistant cells when AMPK was activated but decreased when AMPK was inhibited (Figure 5E).

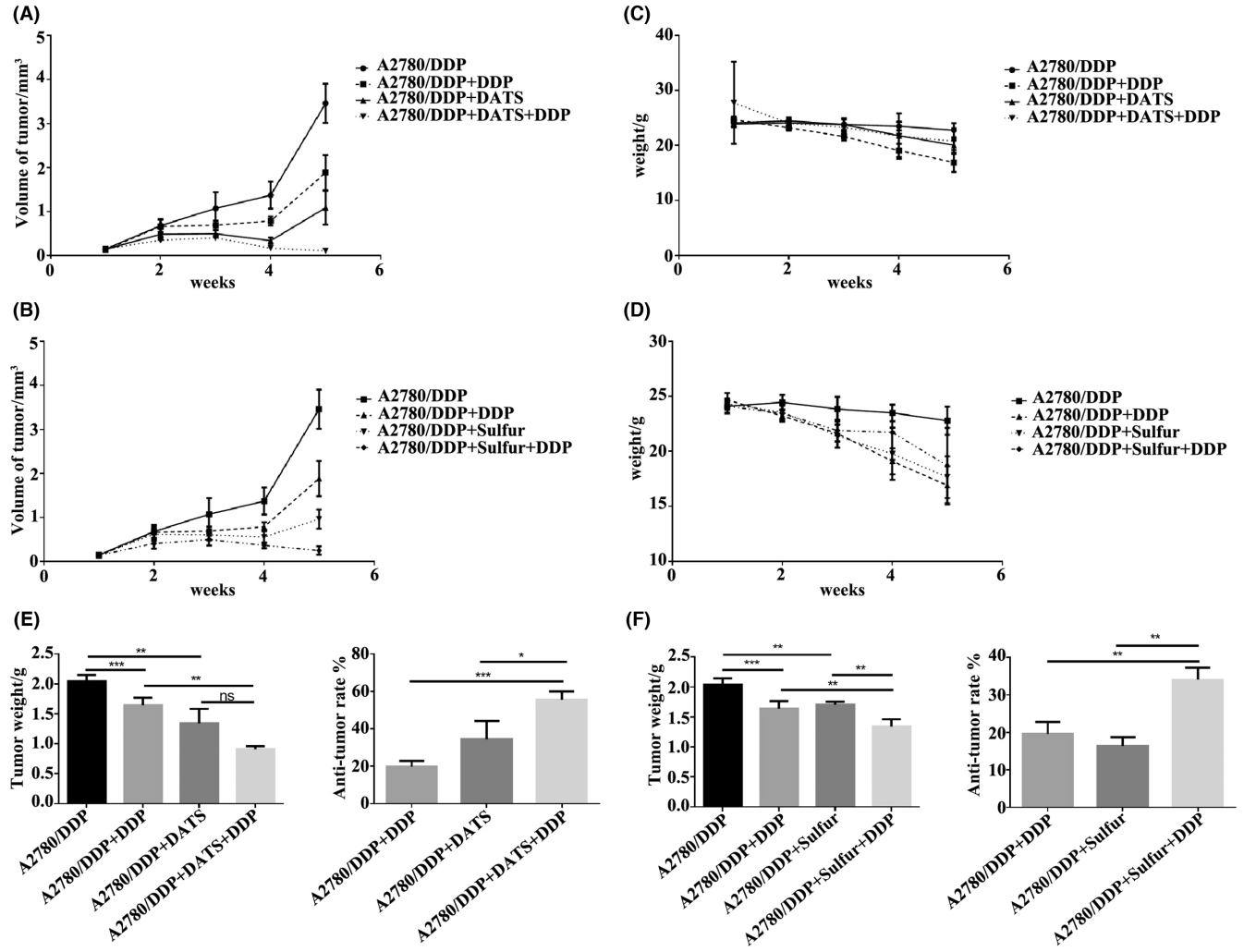

FIGURE 7 Acceleration of tumor size reduction in cisplatin-resistant animal models by sulfur or diallyl trisulfide (DATS). A, B, The volume of tumors. C, D, The weight of mice. E, Tumor weight and antitumor rate after combined treatment with DATS and DDP. F, Tumor weight and antitumor rate after combined treatment with sulfur and DDP. *$p < 0.05$; **$p < 0.01$; ***$p < 0.001$. ns, no significant difference.

3.6 | Requirement of AMPK and PGC-1α for DATS activity in cisplatin-resistant ovarian cancer cells

We transfected cells with PGC-1α siRNA, which decreased PGC1α expression (Figure 6A). As shown in Figure 6B, the inhibition of AMPK protein and knockdown of PGC1α protein significantly affected the DATS upregulatory effect on the total OXPHOS protein expression. It also reversed the DATS-induced increase in ROS levels (Figure 6C). In addition, the effect of DATS on cell viability and apoptosis induction was significantly reduced (Figure 6D,E).

3.7 | Higher effectiveness of DATS in accelerating tumor size reduction than sulfur in cisplatin-resistant animal models

Sulfur is a dietary supplement used for different clinical applications, mostly known for its anti-inflammatory properties and ability to act against tumor cells.[25,26] Sulfur-based compounds have also been used to reduce platinum toxicity.[27] We used sulfur as a positive control to assess the cytotoxicity of DATS in reducing tumor progression of a cisplatin-resistant animal model. Both DATS and sulfur decreased tumor volume and mouse weight, compared with A2780/DDP and the control groups, in the cisplatin-resistant animal model (Figure 7A-D). Therefore, the tumor size was significantly decreased in the animals treated with DATS + DDP or sulfur + DDP compared with DDP alone (Figure 7E,F).

3.8 | DATS can alter tumor morphology, increase the apoptotic cell rate, and inhibit tumor cell proliferation

As shown in Figure 8A,B, the structure of tumor cells in untreated A2780/DDP mice was dense. Compared with mice in the control group, the tumor cells of mice treated with cisplatin, DATS, and sulfur were looser. A larger redstained area within the examined specimen of the mice that were administered cisplatin combined with DATS

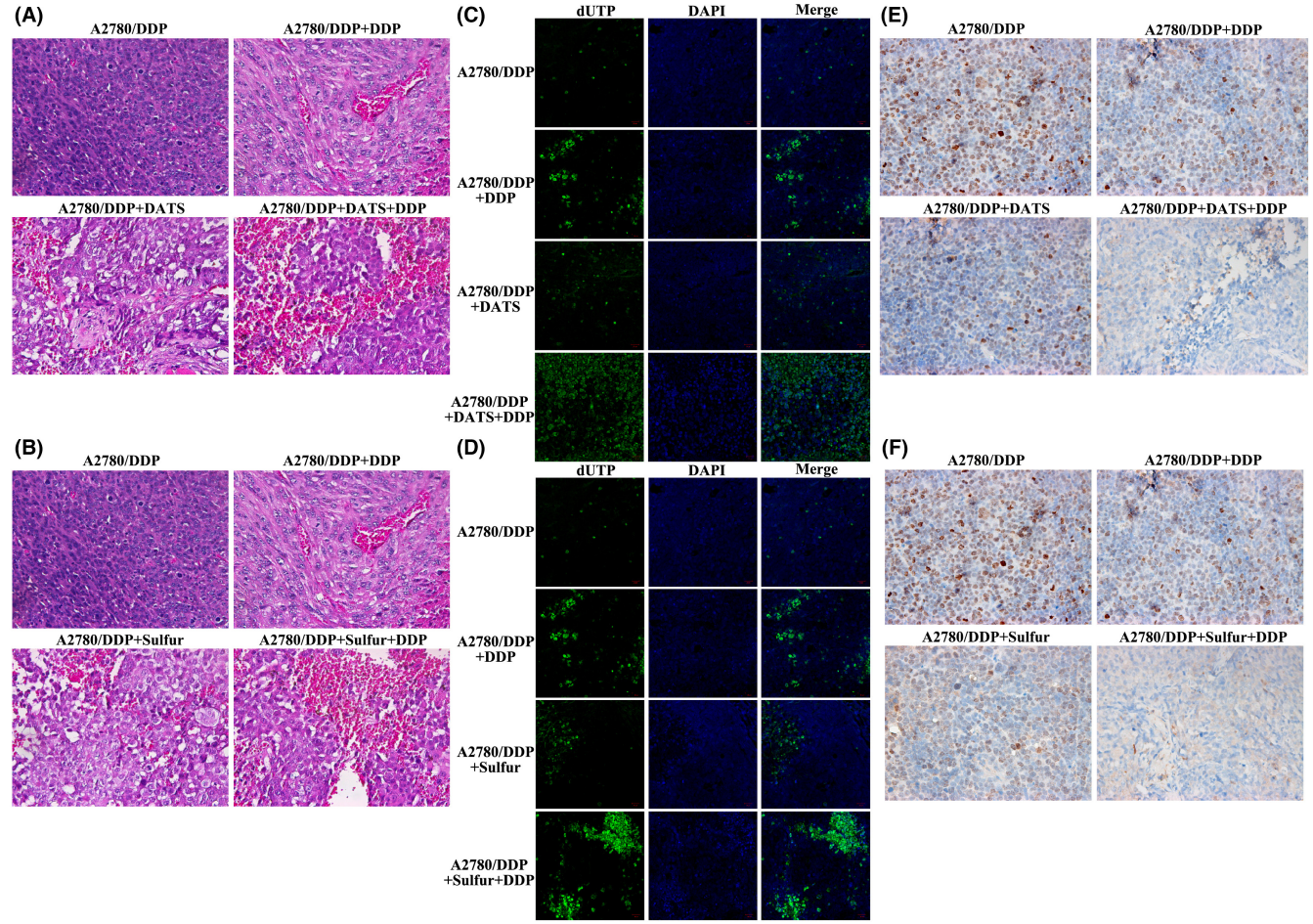

FIGURE 8 Diallyl trisulfide (DATS) can alter tumor morphology, increase the apoptotic cell rate, and inhibit tumor cell proliferation. A, B, Histological analysis of tumor structure was performed using HE staining. C, D, 4UTP-positive cells detected using immunofluorescence assay. E, F, Ki67 expression determined using immunohistochemistry assay.

or sulfur indicated a significant increase in fragmentation. These results indicate that DATS or sulfur can promote the destruction of cisplatin in tumor tissues. As visible in Figure 8C,D, the combination of DATS or sulfur and DDP significantly increased the apoptotic rate compared with the DATS group or sulfur group alone. This result indicated that DATS/sulfur could promote cisplatin-induced apoptosis in tumor tissues. In addition, the significant decrease in ki67 expression in the DATS + DDP and sulfur + DDP groups compared with the DDP group indicated that DATS/sulfur can further enhance the inhibitory effect of cisplatin on the proliferation of tumor tissue cells (Figure 8E,F).

3.9 | DATS or sulfur promotes the activation of the AMPK/SIRT1/PGC1α signaling pathway and upregulates OXPHOS expression

As shown in Figure 9A,B, there was no significant difference in AMPK expression in each group compared with mice in the A2780/DDP group. The pAMPK/AMPK ratio, SIRT1, and total OXPHOS expression in mouse tumor tissues treated with cisplatin, DATS, and sulfur were upregulated compared with the mice in the cisplatin-alone group, and the pAMPK/AMPK ratio, SIRT1, and total OXPHOS levels were increased in the tumor tissues of the mice in the cisplatin + DATS and cisplatin + sulfur combined group. This result indicated that DATS could promote the activity of the AMPK/SIRT pathway and promote the level of OXPHOS, similar to sulfur. In Figure 9C,D, the expression of PGC1α in each group did not change significantly. At the same time, the acetylation of PGC1α has been significantly reduced in the mice treated with DATS or sulfur alone. DDP combined with DATS and sulfur further reduced the acetylation of PGC1α. These results indicated that DATS or sulfur combined with DDP could inhibit PGC1α acetylation.

4 | DISCUSSION

Chemotherapeutic drugs mainly function by inducing cell apoptosis. There are several reasons for the failure of these drugs in clinical application, such as drug resistance or high toxicity against healthy cells. There are classical pathways in which small molecules are targeted for the treatment of various types of cancer. Apoptosis is a

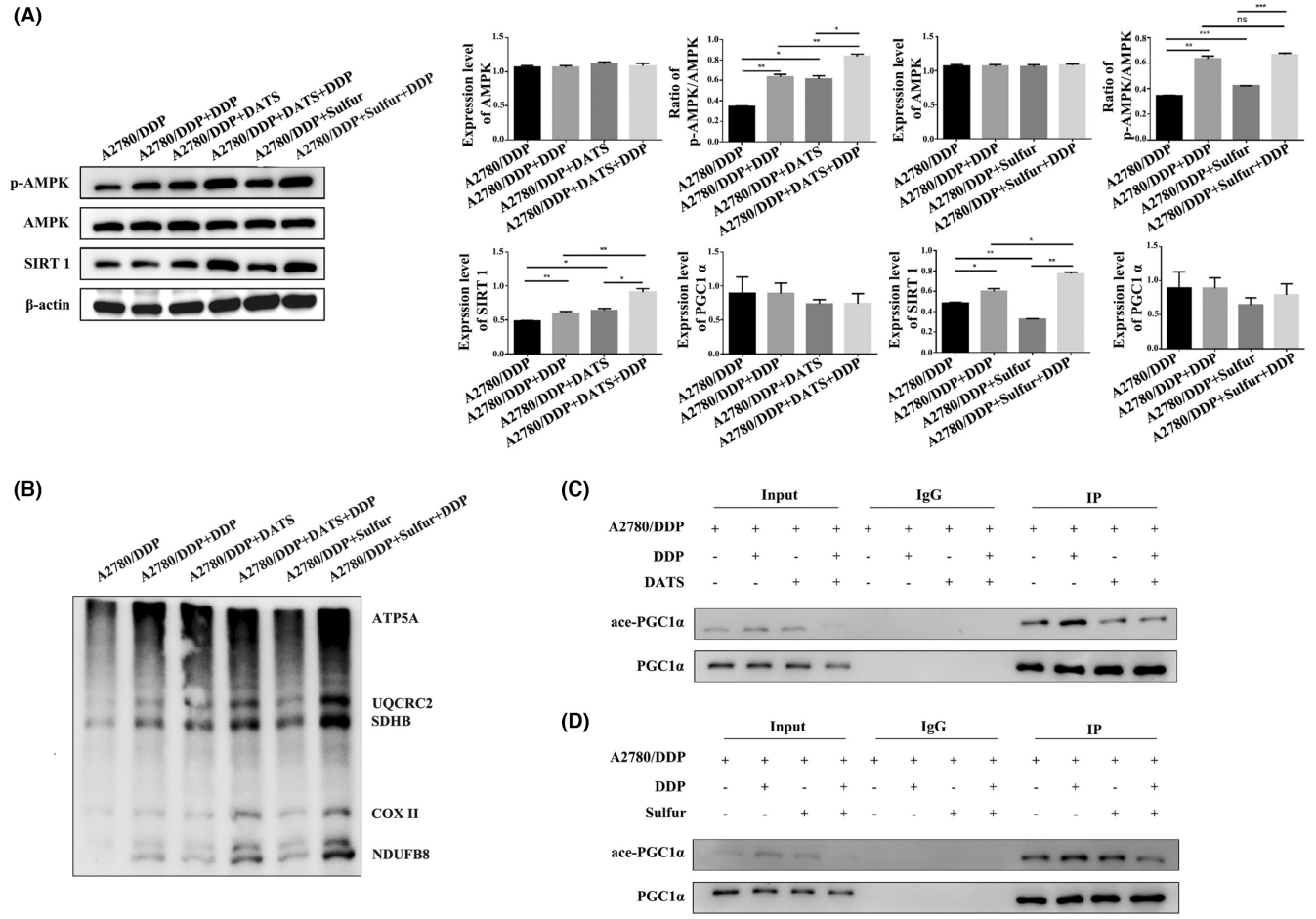

FIGURE 9 Diallyl trisulfide (DATS) or sulfur promotes the activation of the AMPK/SIRT1/PGC1α signaling pathway and upregulates oxidative phosphorylation (OXPHOS) expression. A, The protein expression of p-AMPK, AMPK, and SIRT1 in A2780/DDP cells treated with DDP combined with DATS or sulfur was detected using Western blot. B, Total OXPHOS was detected by Western blot. C, D, The protein expression of PGC1α acetylation in A2780/DDP cells treated with DDP combined with DATS or sulfur was detected using Western blot followed by immunoprecipitation (IP) assay. $^{*}p<0.05$, $^{**}p<0.01$, $^{***}p<0.001$. ns, no significant difference.

well-known cellular mechanism that has been targeted in cancer treatment, and the mitochondrial apoptotic pathway is one of the classical pathways of apoptosis. Enhancing apoptosis is a promising anticancer strategy aimed at reducing tumor progression. DATS can induce cell apoptosis and suppress the growth of cisplatin-sensitive and cisplatin-resistant cells. It has been suggested that DATS may act by promoting cell death signals in response to DNA damage, oxidative stress, and cellular damage. ROS generation is also known to induce apoptosis.[28–32] ROS are produced as a result of normal mitochondrial energy metabolism. When transiently or moderately increased, ROS can activate signaling pathways in response to different types of (metabolic) stress. One of these pathways is the stimulation of glucose uptake. When the ROS levels are altered for a prolonged time, a vicious circle of ROS-stimulated glucose uptake and glucose-stimulated ROS production can be triggered. The alteration of glucose metabolism is characterized by increased uptake of glucose, hyperactivated glycolysis, and decreased OXPHOS component.[33] However, glutamine replaces glucose as the main source of NAPDH production in the absence of glucose. Glutamine has antioxidant effects, and a decrease in its level weakens antioxidant capacity and increases ROS.[34] We found that DATS increased ROS levels and the consumption of glucose and glutamine, suggesting that DATS promoted cell apoptosis by reducing antioxidant capacity; these results are consistent with those of previous studies.[30,35,36]

Recently, it has been shown that the PGC-1α and AMPK-SIRT1 pathways are associated with the regulation of energy metabolism and mitochondrial biogenesis.[15] The link between the AMPK/SIRT1/PGC1α signaling pathway and ovarian cancer is yet to be studied. DATS has been previously reported to induce apoptosis in SKOV-3/DDP ovarian cancer cells via downregulation of PUMA.[14] In the present study, we found that DATS inhibited the growth of both cisplatin-sensitive and cisplatin-resistant ovarian cancer cells. It also reduced IC_{50} and indicated that DATS could be a promising molecule for the treatment of ovarian cancer. Subsequently, we observed that DATS upregulated the AMPK/SIRT1/PGC1α signaling pathway. We examined DATS-induced cell death in cisplatin-resistant ovarian cancer cells using the AMPK/SIRT1/PGC1α signaling pathway. DATS requires AMPK and PGC1α proteins for its activity, while attenuation

of any of these proteins can reverse its effect. These results indicate that the AMPK/SIRT1/PGC1α signaling pathway is crucial for DATS to efficiently overcome cisplatin drug resistance. SIRT1 belongs to the sirtuin family of protein deacetylases. The different deacetylation substrates endow SIRT1 with multiple biological functions.[37] Therefore, we explored the effects of DATS on PGC1α acetylation. The results showed that DATs inhibited the acetylation of PGC1α, suggesting the important role of PGC1α in the regulation of DATS in cisplatin resistance.

Previously, sulfur has been considered an essential dietary supplement that can facilitate cancer chemotherapy due to its antitumor and antioxidant characteristics.[25–27] We administered cisplatin-resistant animal models with a combination of DATS or sulfur and DDP. The results showed that DATS accelerate tumor size and body weight reduction in the presence of DDP, which is similar to the combination of DDP and sulfur. The in vivo results indicated that DATS significantly overcame cisplatin resistance in cisplatin-resistant animal models. DATS appeared to target the OXPHOS process, promoted cell apoptosis, and inhibited cell proliferation. The AMPK/SIRT1/PGC1α signaling pathway is a newly identified target of DATS. Therefore, it is essential to investigate the association between the AMPK protein and PGC1α acetylation modification by DATS and its effect on DATS-mediated cisplatin resistance. Further such studies are warranted to better understand ovarian drug resistance and the most appropriate treatment strategies. Our data suggest a potential signaling pathway target to overcome drug resistance in ovarian cancer and highlight the exact mechanism of DATS, which will help in future studies to develop better treatments for different types of drug-resistant cancer.

There is limited information regarding the PGC1α and AMPK-SIRT1 pathways from a therapeutic perspective. However, our research concluded that DATS is efficient in overcoming cisplatin-resistant ovarian cancer in vivo and in vitro by upregulating the AMPK/SIRT1/PGC1α signaling pathway, increasing ROS levels, and inducing cell apoptosis. We have elucidated that AMPK and PGC1α proteins are essential for DATS activity, and the combination of DATS and sulfur treatment in vivo significantly reduced the animals' tumor volume and body weight. Our data suggest a novel mechanism for DATS, which can be considered a novel strategy for the treatment of drug-resistant ovarian cancer. It also provides new insights into the correlation between AMPK and PGC1α and their potential as targets in cancer therapy.

ACKNOWLEDGMENT

This research was supported by the National Natural Science Foundation of China under grant number 81260531 and 81873268.

DISCLOSURE

The authors declare no conflict of interest.

DATA AVAILABILITY STATEMENT

The datasets used and analyzed during the current study are available from the corresponding author on reasonable request.

ETHICS STATEMENT

None.

Approval of the research protocol by an Institutional Reviewer Board: N/A.

Informed Consent: N/A.

Registry and the Registration No. of the study/trial: N/A.

Animal Studies: None.

ORCID

Yunxi Ji https://orcid.org/0000-0001-9753-8154

REFERENCES

1. Li M, Balch C, Montgomery JS, et al. Integrated analysis of DNA methylation and gene expression reveals specific signaling pathways associated with platinum resistance in ovarian cancer. *BMC Med Genomics*. 2009;2:34.
2. Ferlay J, Soerjomataram I, Dikshit R, et al. Cancer incidence and mortality worldwide: sources, methods and major patterns in GLOBOCAN 2012. *Int J Cancer*. 2015;136:E359-E386.
3. Webb PM, Jordan SJ. Epidemiology of epithelial ovarian cancer. *Best Pract Res Clin Obstet Gynaecol*. 2017;41:3-14.
4. Lengyel E, Burdette JE, Kenny HA, et al. Epithelial ovarian cancer experimental models. *Oncogene*. 2014;33:3619-3633.
5. Bast RC Jr, Hennessy B, Mills GB. The biology of ovarian cancer: new opportunities for translation. *Nat Rev Cancer*. 2009;9:415-428.
6. Dasari S, Tchounwou PB. Cisplatin in cancer therapy: molecular mechanisms of action. *Eur J Pharmacol*. 2014;740:364-378.
7. Liu X, Gao Y, Lu Y, Zhang J, Li L, Yin F. Oncogenes associated with drug resistance in ovarian cancer. *J Cancer Res Clin Oncol*. 2015;141:381-395.
8. Puccinelli MT, Stan SD. Dietary bioactive diallyl trisulfide in cancer prevention and treatment. *Int J Mol Sci*. 2017;18:1645.
9. Altonsy MO, Andrews SC. Diallyl disulphide, a beneficial component of garlic oil, causes a redistribution of cell-cycle growth phases, induces apoptosis, and enhances butyrate-induced apoptosis in colorectal adenocarcinoma cells (HT-29). *Nutr Cancer*. 2011;63:1104-1113.
10. Fleischauer AT, Arab L. Garlic and cancer: a critical review of the epidemiologic literature. *J Nutr*. 2001;131:1032S-1040S.
11. Lee JE, Lee RA, Kim KH, Lee JH. Induction of apoptosis with diallyl disulfide in AGS gastric cancer cell line. *J Korean Surg Soc*. 2011;81:85-95.
12. Li W, Tian H, Li L, et al. Diallyl trisulfide induces apoptosis and inhibits proliferation of A549 cells in vitro and in vivo. *Acta Biochim Biophys Sin (Shanghai)*. 2012;44:577-583.
13. Tu S, Liu ZQ, Fu JJ, Zhu WF, Luo DY, Wan FS. Inhibitory effect of p53 upregulated modulator of apoptosis targeting siRNA on hypoxia/reoxygenation-induced cardiomyocyte apoptosis in rats. *Cardiology*. 2012;122:93-100.
14. Wan HF, Yu LH, Wu JL, et al. Effect of diallyl trisulfide on human ovarian cancer SKOV- 3/DDP cell apoptosis. *Asian Pac J Cancer Prev*. 2013;14:7197-7201.
15. Thirupathi A, de Souza CT. Multi-regulatory network of ROS: the interconnection of ROS, PGC-1 alpha, and AMPK-SIRT1 during exercise. *J Physiol Biochem*. 2017;73:487-494.
16. Zhang Y, Ba Y, Liu C, et al. PGC-1alpha induces apoptosis in human epithelial ovarian cancer cells through a PPARgamma-dependent pathway. *Cell Res*. 2007;17:363-373.
17. Liemburg-Apers DC, Willems PH, Koopman WJ, Grefte S. Interactions between mitochondrial reactive oxygen species and cellular glucose metabolism. *Arch Toxicol*. 2015;89:1209-1226.

18. Quinlan CL, Perevoshchikova IV, Hey-Mogensen M, Orr AL, Brand MD. Sites of reactive oxygen species generation by mitochondria oxidizing different substrates. *Redox Biol*. 2013;1:304-312.
19. Quinlan CL, Treberg JR, Perevoshchikova IV, Orr AL, Brand MD. Native rates of superoxide production from multiple sites in isolated mitochondria measured using endogenous reporters. *Free Radic Biol Med*. 2012;53:1807-1817.
20. Mailloux RJ, Jin X, Willmore WG. Redox regulation of mitochondrial function with emphasis on cysteine oxidation reactions. *Redox Biol*. 2014;2:123-139.
21. Galloway CA, Yoon Y. Perspectives on: SGP symposium on mitochondrial physiology and medicine: what comes first, misshape or dysfunction? The view from metabolic excess. *J Gen Physiol*. 2012;139:455-463.
22. Brown JAL. In vitro histone acetylation assay. *Curr Protoc Pharmacol*. 2017;79:3 14 11-13 14 16.
23. Mastropasqua F, Girolimetti G, Shoshan M. PGC1alpha: friend or foe in cancer? *Genes (Basel)*. 2018;9:48.
24. Bost F, Kaminski L. The metabolic modulator PGC-1alpha in cancer. *Am J Cancer Res*. 2019;9:198-211.
25. Kowalska K, Habrowska-Gorczynska DE, Dominska K, Urbanek KA, Piastowska-Ciesielska AW. Methylsulfonylmethane (organic sulfur) induces apoptosis and decreases invasiveness of prostate cancer cells. *Environ Toxicol Pharmacol*. 2018;64:101-111.
26. P.N. S, Darvin P, Yoo YB, et al. The combination of methylsulfonylmethane and tamoxifen inhibits the Jak2/STAT5b pathway and synergistically inhibits tumor growth and metastasis in ER-positive breast cancer xenografts. *BMC Cancer*. 2015;15:474.
27. Dedon PC, Borch RF. Characterization of the reactions of platinum antitumor agents with biologic and nonbiologic sulfur-containing nucleophiles. *Biochem Pharmacol*. 1987;36:1955-1964.
28. Das A, Banik NL, Ray SK. Garlic compounds generate reactive oxygen species leading to activation of stress kinases and cysteine proteases for apoptosis in human glioblastoma T98G and U87MG cells. *Cancer*. 2007;110:1083-1095.
29. Kim YA, Xiao D, Xiao H, et al. Mitochondria-mediated apoptosis by diallyl trisulfide in human prostate cancer cells is associated with generation of reactive oxygen species and regulated by Bax/Bak. *Mol Cancer Ther*. 2007;6:1599-1609.
30. Na HK, Kim EH, Choi MA, Park JM, Kim DH, Surh YJ. Diallyl trisulfide induces apoptosis in human breast cancer cells through ROS-mediated activation of JNK and AP-1. *Biochem Pharmacol*. 2012;84:1241-1250.
31. Wang HC, Yang JH, Hsieh SC, Sheen LY. Allyl sulfides inhibit cell growth of skin cancer cells through induction of DNA damage mediated G2/M arrest and apoptosis. *J Agric Food Chem*. 2010;58:7096-7103.
32. Wu XJ, Hu Y, Lamy E, Mersch-Sundermann V. Apoptosis induction in human lung adenocarcinoma cells by oil-soluble allyl sulfides: triggers, pathways, and modulators. *Environ Mol Mutagen*. 2009;50:266-275.
33. Cruz-Bermúdez A, Laza-Briviesca R, Vicente-Blanco RJ, et al. Cisplatin resistance involves a metabolic reprogramming through ROS and PGC-1α in NSCLC which can be overcome by OXPHOS inhibition. *Free Radic Biol Med*. 2019;135:167-181.
34. Hayes JD, Dinkova-Kostova AT, Tew KD. Oxidative stress in cancer. *Cancer Cell*. 2020;38:167-197.
35. Kim SH, Bommareddy A, Singh SV. Garlic constituent diallyl trisulfide suppresses x-linked inhibitor of apoptosis protein in prostate cancer cells in culture and in vivo. *Cancer Prev Res (Phila)*. 2011;4:897-906.
36. Oommen S, Anto RJ, Srinivas G, Karunagaran D. Allicin (from garlic) induces caspase-mediated apoptosis in cancer cells. *Eur J Pharmacol*. 2004;485:97-103.
37. Zhang W, Feng Y, Guo Q, et al. SIRT1 modulates cell cycle progression by regulating CHK2 acetylation-phosphorylation. *Cell Death Differ*. 2020;27:482-496.

How to cite this article: Wang Z, Yan Y, Lou Y, et al. Diallyl trisulfide alleviates chemotherapy sensitivity of ovarian cancer via the AMPK/SIRT1/PGC1α pathway. *Cancer Sci*. 2023;114:357-369. doi: 10.1111/cas.15627